CONCLUSION

The pattern of the physiological distribution of FDG within laryngeal muscle during phonation is important to recognize to enable differentiation of physiological from pathological uptake, particularly in the assessment of patients with head and neck tumors. The uptake in laryngeal muscles may have future application for the investigation of patients with speech disorders.

REFERENCES

1. Frey LD, Locher JT, Hrycaj P, Stratz T, Kovac C, Mennet P, Muller W. Determination of regional rate of glucose metabolism in lumbar muscles in patients with generalized tendomyopathy using dynamic FDG-PET. *Z Rheumatol* 1992;5:238–242.
2. Mossberg KA, Mommessin JI, Taegtmeyer H. Skeletal muscle glucose uptake during short-term contractile activity in vivo: effect of prior contractions. *Metabolism* 1993;42:1609–1616.
3. Barrington SF, Maisey MN. Skeletal muscle uptake of ^{18}FDG: the effect of oral diazepam in tense patients. *J Nucl Med* 1996;37:1127–1129.
4. Hamacher K, Coenen HH, Stocklin G. Efficient stereospecific synthesis of no-carrier-added 2-[^{18}F] fluoro-2-deoxyglucose using aminopolyether supporter nucleophilic substitution. *J Nucl Med* 1986;27:235–238.
5. Hawkes DJ, Ruff CF, Hill DLG, et al. Three-dimensional mutlimodality imaging in image-guided interventions. *Semin Interv Radiology* 1995;12:63–74.
6. Jabour BA, Choi Y, Hoh CK, et al. Extracranial head and neck PET imaging with 2-[^{18}F]fluoro-2-deoxy-D-glucose and MR imaging correlation. *Radiology* 1993;86:27–35.
7. Rege S, Maas A, Chaiken L, et al. Use of positron emission tomography with fluorodeoxyglucose in patients with extracranial head and neck cancers. *Cancer* 1994;73:3047–3058.
8. Zeitouni AG, Yamamoto YL, Black M, Gjedde A. Functional imaging of head and neck tumors using positron emission tomography. *J Otolaryngol* 1994;23:77–80.

Advantages of SPECT in Technetium-99m-Sestamibi Parathyroid Scintigraphy

Claire Billotey, Emile Sarfati, André Aurengo, Michéle Duet, Olivier Mündler, Marie-Elisabeth Toubert, Jean-Didier Rain and Yves Najean

Departments of Nuclear Medicine and General Surgery, Hôpital Saint-Louis; Department of Nuclear Medicine, Hôpital de la Pitié; and Department of Nuclear Medicine, Hôpital Lariboisière, Paris, France

We demonstrate several advantages of SPECT in parathyroid scintigraphy. **Methods:** Forty-four parathyroid ^{99m}Tc-MIBI scintigrams were obtained before surgery in 43 patients suffering from hyperparathyroidism. For each patient, we obtained dynamic views and planar and SPECT images of the neck and thorax. For 15 patients, we also acquired a delayed static view of the neck 2 hr after tracer injection. Abnormal thyroid-area glands were detected with factor analysis of dynamic structure (FADS) of the initial dynamic acquisition. In the 15 patients with delayed views of the neck, we compared FADS and the double-phase study results to detect glands in the thyroid uptake area. Glands outside the thyroid area were demonstrated on planar views. The location of enlarged glands was more precisely defined on the tomographic slices. The anatomic and histologic findings and the evolution of hypercalcemia after surgery were taken as reference. **Results:** Sixty-four abnormal glands were found during surgery, including 39 observed in patients who underwent reoperation for persistent or recurrent hyperparathyroidism. Twenty-two of these glands were in an abnormal location, including 10 in the mediastinum. SPECT allowed the detection of three glands not demonstrated on planar views or FADS. Fifty-eight glands were correctly localized scintigraphically, including 34 in patients who underwent reoperation. Therefore, SPECT raised the sensitivity from 86% to 90.5% and from 79.5% to 87% in the reoperated patients. Tracer uptake in the low mediastinal area was better analyzed on tomographic slices than on planar views. Only seven false-positive results were depicted by planar views or FADS; none were depicted on SPECT. **Conclusion:** A combination of FADS and SPECT permits detection of small glands, even in a posterior location, inside or outside the thyroid area. This scintigraphic method enables the surgeon to define more precisely details about the location of the enlarged gland and contributes to improved parathyroid surgery.

Key Words: parathyroid scintigraphy; technetium-99m-sestamibi; SPECT; FADS

J Nucl Med 1996; 37:1773–1778

Expert parathyroid surgeons can cure 95% or more patients with hyperparathyroidism, even without any preoperative localization study, in cases of primary surgery (*1,2*). In contrast, parathyroid surgery for recurrent or persistent hyperparathyroidism, is much more difficult (*3,4*) and less successful. Granberg et al. (*5*) calculated a surgical success rate of 85% in a compilation of 550 reoperated patients.

In the case of reoperation for persistent or recurrent hyperparathyroidism, the proportion of glands at unusual sites is large: 72% in a series of 112 reoperations (*6*) and a cumulative

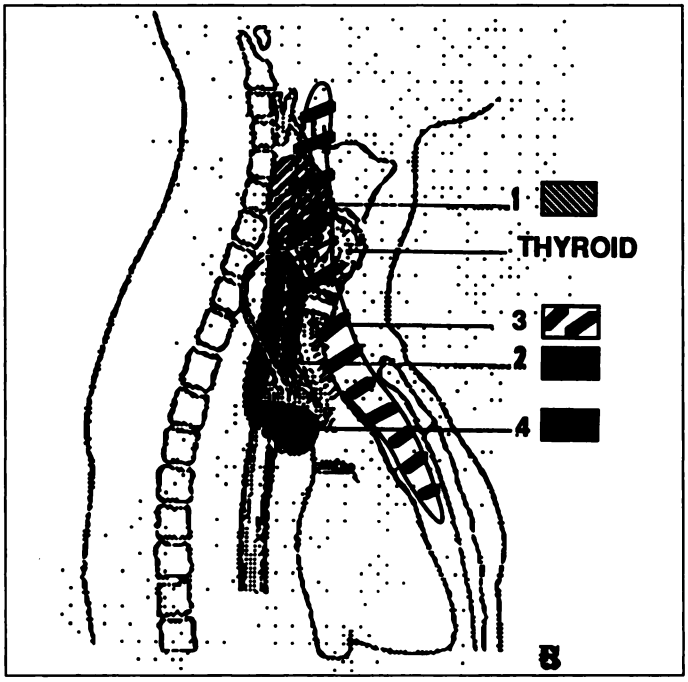

FIGURE 1. Localization of (1) normal and (2) abnormal posterosuperior glands and (3) anteroinferior glands. (4) Middle mediastinum area.

Received March 29, 1996; revision accepted April 1, 1996.

For correspondence or reprints contact: Dr. Claire Billotey, Service de Médecine Nucléaire, Hôpital Saint-Louis, 1 Av Claude Vellefaux, 75450 Paris, Cedex 10, France.

TABLE 1
Patients with Each Type of Hyperparathyroidism (HPT)

	Type of HPT			
	Primary	Secondary	Tertiary	Total
First surgery	5	4	1	10
Reoperation	19	12	2	33
Total	24	16	3	43

rate of 58% for six series with a total of 253 abnormal glands (*3,5–9*). The abnormal sites vary considerably. They may be cervical, cervico-mediastinal or purely mediastinal, either anterior or very posterior (Fig. 1).

The exact location of residual parathyroid tissue is important to the surgeon, especially for mediastinal glands which constitute about 20% of the patients in a series of 112 (*6*). In such patients, the glands are frequently anterior, right at the back of the sternal plane, often in a thymus persistens and sometimes in the great vessel area under the aortic arch, an area called the middle mediastinum (Fig. 1), or still further behind (latero-oesophageal). Such sites make detection difficult with planar views.

As early as 1974, several tomographic scintigraphic methods were proposed (*10–14*), but their sensitivity was low (*15*). In 1979 and 1980, many authors recorded the advantages of multiple-slice acquisitions and multiplane data reconstruction, using a single detector equipped with a parallel-hole (*16*) or a convergent beam collimator (*17*). The principal advantage is the improvement of contrast enhancement (*18*). The recent advances in new radiopharmaceuticals, instrumentation, data acquisition, image reconstruction and processing techniques allow the use of SPECT in clinical practice.

We have demonstrated that factor analysis of dynamic structures (FADS) is a good method for detecting abnormal parathyroid glands in the thyroid uptake area (*19*). FADS appears to better identify particularly hyperplastic glands than a method based on acquisition of a delayed view (double-phase method). To detect abnormal parathyroid glands localized in the thyroid uptake area, SPECT was associated with only FADS. To detect glands outside the thyroid uptake area, SPECT was combined with planar imaging.

We postulated that information allowing more precise localization of abnormal parathyroid glands would facilitate surgical procedures. The aim of the present study, therefore, was to evaluate the advantages of SPECT in the detection of these glands, particularly in patients undergoing reoperation, using ^{99m}Tc-MIBI as a tracer.

MATERIALS AND METHODS

Patients

Forty-four parathyroid scintigrams were obtained from 43 patients. All patients had patent biological signs of hyperparathyroidism (high serum calcium and enhanced or inappropriate intact 1–84 parathormone levels). Three types of hyperparathyroidism were observed (Table 1). Ten patients were operated on for the first time and 33 patients underwent reoperation. Fourteen patients had a thyroid nodule or multinodular goiter and four had previous total or partial thyroidectomies. All patients had surgery from 1 day to 4 mo after scintigraphy. Five patients had scintigraphy 1 or 2 days after previous unsuccessful surgical neck exploration and were reoperated on within 24 hr. One patient had two scintigraphic sessions with each realized before one productive reoperation.

Sixty-four abnormal glands were found during surgery. They comprised 17 adenomas (including one lipoadenoma) and 47 hyperplastic glands. They were located at various sites and included 10 glands in the mediastinum and two in the forearm wich corresponded to hyperplasia of a parathyroid graft (Table 2). In one patient, no abnormal gland was found during surgery, and the hyperparathyroidism persisted. In 16 patients, who were on dialysis for kidney failure, the abnormal serum parathormone level was corrected on the 15th day after surgery. In all the other patients, calcemia returned to normal during the first 24 hr postoperatively. The overall success rate of reoperation was 97% (33 of 34 patients). There were no deaths from surgery and morbidity was limited to a few cases of transient hypocalcemia.

Data Acquisition

We used a circular large field of view gamma camera. The patients fasted for at least 4 hr before imaging and were immobilized in the supine position with the head and neck extended. We injected a bolus containing 400 to 750 MBq ^{99m}Tc-MIBI (10–20 mCi), labeled according to the manufacturer's instructions. An initial 30-min period of dynamic aquisition started immediately after the bolus injection. Acquisition was performed with a pinhole collimator centered on the thyroid area and consisted of 25 to 30 one-minute 64 × 64 or 128 × 128 frames. A second set of data was then acquired, using a low-energy, high-resolution parallel collimator. We began by performing planar imaging of the neck (lateral views, 1.5 to 2 zoom acquisition factor, 128 × 128 matrix, 600 kcts) and then of the thorax (anterior incidence, 128 × 128 matrix, 800 kcts). If the patient had a previous parathyroid graft in the forearm, images were also made of both forearms (128 × 128 matrix, 400 kcts). Lastly, in all patients, we acquired SPECT images of the neck and thorax with an elliptical orbit of 360° using a 64 × 64 matrix and 64 steps per 55 sec. Barium-133 markers were placed on the sternal manubrium.

In 15 patients, a delayed anterior thorax planar view (128 × 128 matrix, 800 kcts) 2 hr after the tracer injection (double-phase method) was also obtained. We also compared FADS with the double-phase study data for detection of abnormal glands in the thyroid uptake area.

Data Processing

The tomographic data were reconstructed by filtered backprojection with a vertical and horizontal Wiener filter. In some patients, a mask was applied to limit the explored area to the neck and mediastinum. For two-slice superposition of the slices, immunoscintigraphy software enabled dual-isotope analysis.

Kinetic of tracer uptake in the thyroid area was analyzed by FADS (Famis® software, Sopha Medical Vision) (*19*). Abnormal parathyroid glands in the thyroid uptake area were so detected by FADS, but, even if FADS showed no parathyroid activity, uptake behind the thyroid uptake area that was visible on the tomographic

TABLE 2
Site and Pathologic Data for 64 Abnormal Glands Removed Surgically

Location				Pathologic examination	
Cervical	Cervicomediastinal	Mediastinal	Forearm	Adenoma	Hyperplasia
47	5	10	2	17	47

TABLE 3
Agreement/Disagreement between FADS and Double-Phase Method (DPM) Results for Detecting Abnormal Parathyroid Glands in Thyroid Uptake Area in 15 Patients Expressed in Each Thyroid Quadrant (n = 58)

	FADS			
DPM	TP	TN	FP	FN
TP	5	–	–	–
TN	–	30	–	–
FP	–	4	1	–
FN	14	–	–	4

TP = true-positive; TN = true-negative; FP = false-positive; FN = false-negative.

slices was considered as abnormal and corresponding to a parathyroid gland.

We interpreted tracer uptake in the mediastinum and neck outside the thyroid uptake area on static planar views and on tomographic sagittal, frontal and transverse slices. All uptake sites except those in the salivary glands and myocardium were considered to be abnormal and to correspond to parathyroid tissue if they were in a known ectopic area (high lateral cervical, low paramedian cervical or mediastinal).

Statistical Analysis

We considered as true-positive each scintigraphic location of abnormal uptake that corresponded to an abnormal parathyroid gland found in the same location by surgery and confirmed by histological examination and evolution of hypercalcemia.

RESULTS

Results and agreement or disagreement between the FADS and the double-phase study are sumarized in Table 3 for the 15 patients on whom we performed both methods to detect abnormal gland(s) in the thyroid uptake area.

In all patients, 55 of the 64 surgically and pathologically proven abnormal glands were correctly detected by scintigraphy. FADS detected 35 of 43 glands localized in the thyroid area and one more was detected by SPECT. The four cervical glands localized outside the thyroid area and 13 cervico-mediastinal, mediastinal glands and hyperplasy of forearm grafts were detected by planar imaging, and two more were detected by SPECT (Table 4). Consequently, the sensitivity of scintigraphy was 90.5% (58/64) for all patients and 87% (34/39) for patients undergoing reoperation.

The three adenomas not detected by FADS or planar imaging were small and/or very posterior. They comprised a cervical

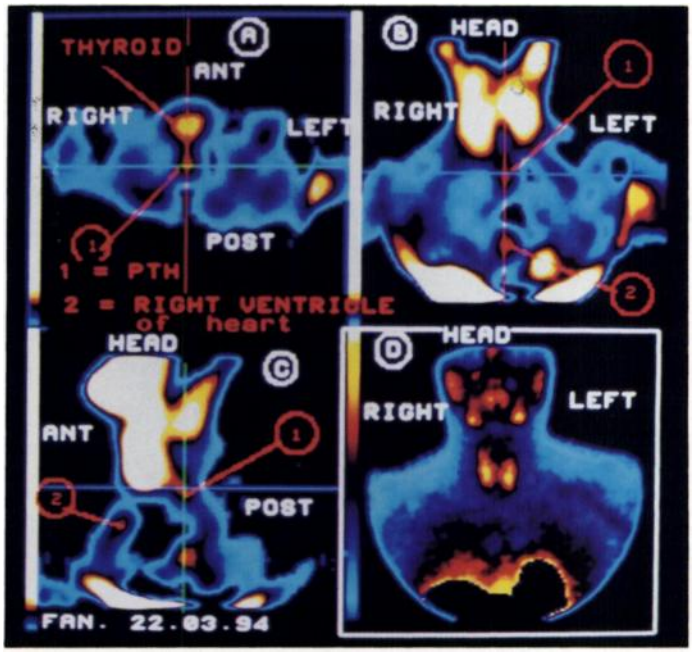

FIGURE 2. Scintigraphic results for a patient suffering from recurrent primary lipoadenomatous hyperparathyroidism that persisted after previous subtotal parathyroidectomy (only half of the right posterosuperior gland was removed): (A) transverse, (B) frontal and (C) sagittal reconstructed tomographic slices and (D) an anterior static view. The abnormal gland was not identified by FADS (false-negative result), but was seen on the tomographic slices. The surgeon found a recurrence of lipoadenomatous hyperparathyroidism on the half right postero-superior gland, which only weighed only 174 mg corresponding to the tomographic image (see the parathyroid gland marked PTH).

adenoma in the thyroid area, weighing 174 mg (Fig. 2), a posterior cervico-mediastinal, 135-mg adenoma and a 700-mg adenoma in the middle mediastinum (Fig. 3). SPECT images for the 10 patients with mediastinal glands showed that the uptake sites were in the anterior mediastinum in seven patients (Fig. 4) and in the middle mediastinum in three patients (Fig. 5). Superposition of radiomarkers in one patient showed MIBI uptake in the anterior mediastinum, a little behind the sternal plane (Fig. 6). This image enabled the surgeon to find the abnormal gland after two previously unsuccessful sternotomies. SPECT images of three of five patients with cervico-mediastinal glands indicated the posterior location (two patients) or anterior (one patient) location of the uptake (Fig. 7). In one patient with a gland located in the thyroid area and detected by FADS, the tomographic slices showed that the thyroidal and parathyroidal uptake extended backwards, suggesting a posterior location of the abnormal parathyroid gland (Fig. 8). This may explain why the US image was negative. In two patients,

TABLE 4
Number of Surgically- and Pathologically-Proven Abnormal Glands* Detected by the Various Methods

		Scintigraphy			
Location	Surgery	FADS (+)	PV (+)	FADS (−) and SPECT (+)	PV (−) and SPECT (+)
In thyroid uptake area	43 (19)	35 (15)		1 (1)	
Outside thyroid uptake area					
Cervical	4 (3)		4 (3)		0
Cervico-med	5 (5)		2 (2)		1 (1)
Mediastinal	10 (10)		9 (9)		1 (1)
Forearm	2 (2)		2 (2)		–

*Glands located in thyroid uptake area and detected by FADS. Glands located in thyroid uptake area and not detected by FADS but by SPECT. Glands outside the thyroid uptake area and detected by planar imaging. Glands not detected on planar views but SPECT. The four cervical glands detected on planar views were outside the thyroid area.

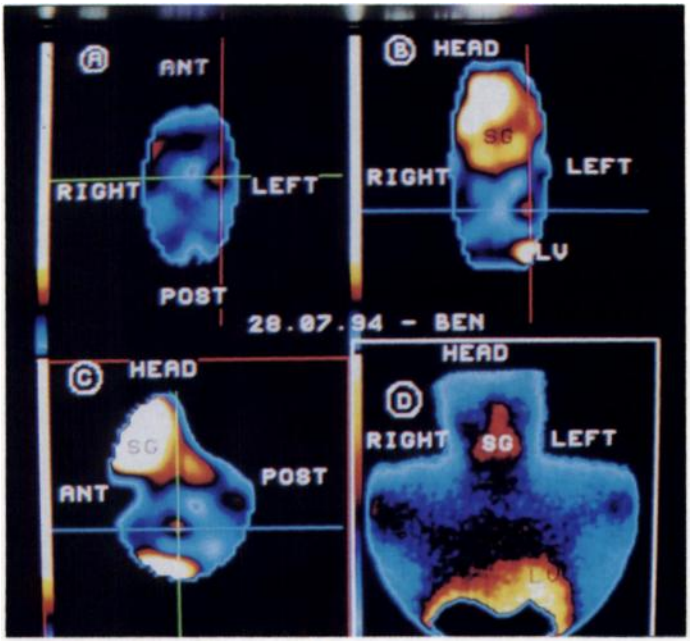

FIGURE 3. Scintigraphic results for a patient with primary hyperparathyroidism which persisted after previous unsuccessful cervicotomy performed 24 hr before scintigraphy. During this cervicotomy, the surgeon found four normal glands. (A) Transverse, (B) frontal and (C) sagittal reconstructed tomographic slices and (D) anterior static view. A 700-mg adenoma was found in the middle mediastinum during reoperation 24 hr later.

a hot spot localized on the right side of the left ventricle looked suspicious due to its focalized character. In one case, two previous imaging tests performed with ^{201}Tl and the other with MIBI had led to the conclusion that the glands were located quite low in the mediastinum. The tomographic slices showed that the thallium uptake was continuous in relation to right myocardial uptake, which was later confirmed surgically.

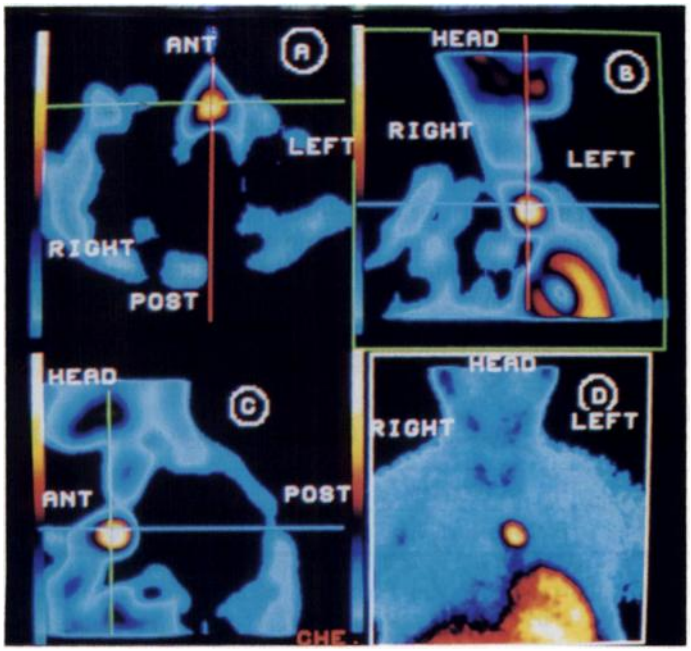

FIGURE 4. Scintigraphic results in a patient with secondary hyperparathyroidism which persisted after one previous operation for the removal of three hyperplastic glands: (A) transverse, (B) frontal and (C) sagittal reconstructed tomographic slices and (D) an anterior static view. A 6-g hyperplastic gland was found during surgery in the left thymus persistent in the anterior mediastinum, which corresponds to the planar and tomographic images. Although this patient had a multinodular goiter, the FADS result was true-negative.

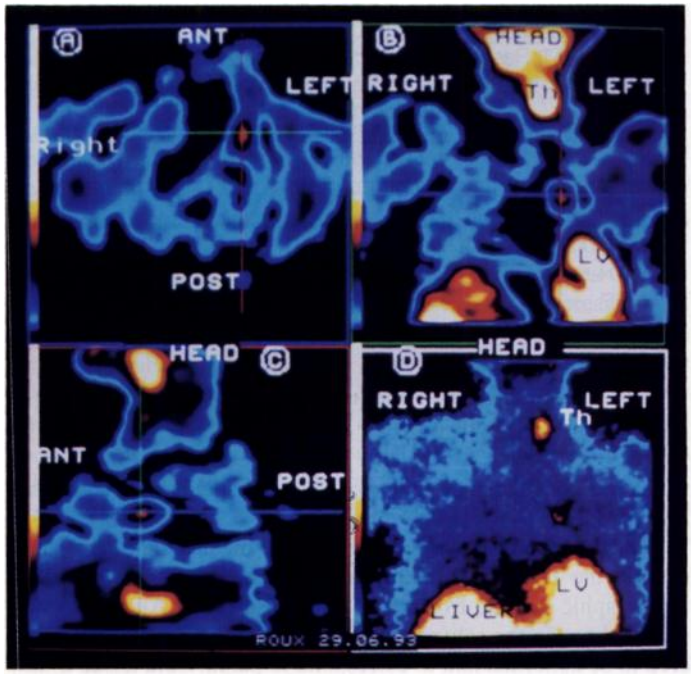

FIGURE 5. Scintigraphic results in a patient with primary hyperparathyroidism persisting after previous cervicotomy found no abnormal gland. (A), Transverse (B) frontal and (C) sagittal reconstructed tomographic slices and (D) anterior static view at 1 hr. One adenoma, weighing 675 mg was found during surgery in the middle mediastinum, which corresponds to the planar and tomographic images.

Five false-positive results were obtained, three from FADS and two from planar views comprising one in the cervicomediastinal area and one in the thorax. In this last patient, uptake was localized on the tomographic slices behind the left ventricle. As this does not correspond to a known localization of an ectopic parathyroid gland, this result must be interpreted cautiously.

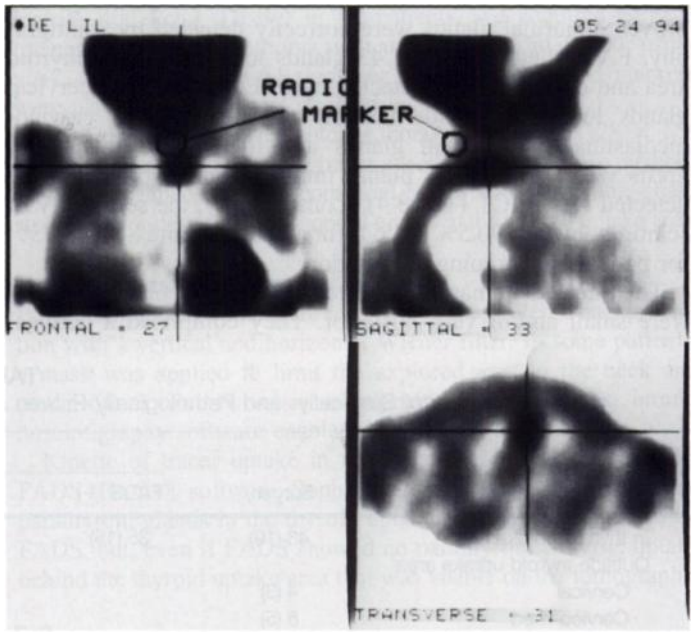

FIGURE 6. Scintigraphic results for a patient with primary hyperparathyroidism that persisted after four previous unsuccessful operations, including two sternotomies and total thyroidectomy: (A) transverse, (B) frontal and (C) sagittal reconstructed tomographic slices, with the superposition of the barium-133 marker on the extremity of the upper sternal manubrium. A 2.4-g gland was found during surgery in a fibrotic area of the anterior mediastinum, on the aortic arch, which corresponds to the planar and tomographic images.

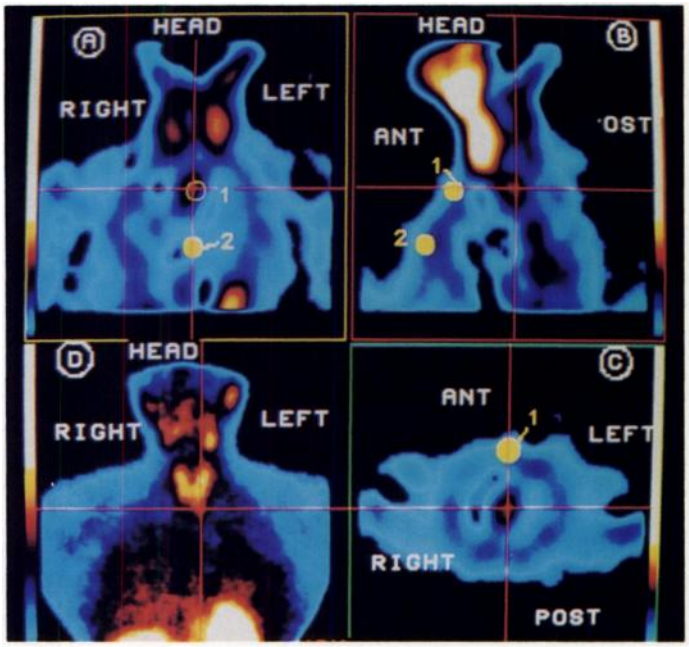

FIGURE 7. Scintigraphic results for a patient with primary hyperparathyroidism which persisted after previous cervicotomy failed to reveal any abnormal gland: (A) transverse, (B) frontal and (C) sagittal reconstructed tomographic slices (D) and anterior static view. A 402-mg left latero-esophageal adenoma was found during further surgery, which corresponds to the planar and tomographic image. Radiomarker 1 was placed on the extremity of the upper sternal manubrium. Radiomarkers 1 and 2 were 7 cm apart.

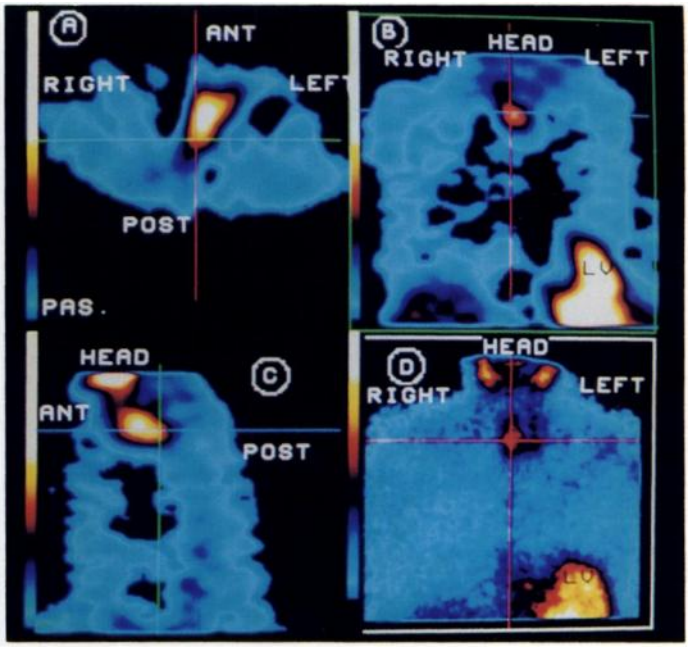

FIGURE 8. Scintigraphic results for a patient with primary hyperparathyroidism. (A) Transverse, (B) frontal and (C) sagittal reconstructed tomographic slices and (D) anterior static view. This patient had previous cervical rachis surgery that ruled out cervical hyperextension. The surgeon therefore needed to know the site of the abnormal gland to perform only a partial cervicotomy. Ultrasonographic exploration was not contributive. FADS analysis enabled detection of one abnormal gland in the area of the right inferior thyroid pole. The tomographic images indicated that this gland was posterior. The surgeon only performed right partial cervicotomy and found a 900-mg, latero-esophageal cervical adenoma. The surgical findings were in good agreement with the scintigraphic results.

DISCUSSION

Coakley (*20*) was the first to suggest using ^{99m}Tc-MIBI for parathyroid imaging in 1989. Although ^{99m}Tc-MIBI uptake is lower than that of ^{201}Tl both in abnormal parathyroid glands and in the thyroid (*21*), several studies (*22,23*) using image subtraction have demonstrated the higher sensitivity of ^{99m}Tc-MIBI compared to ^{201}Tl, possibly because of the better detectability of ^{99m}Tc. However, the gain in sensitivity obtained with ^{99m}Tc-MIBI using these conventional subtraction methods (*21–23*) was modest.

We recently proposed a new method of single-tracer scintigraphy that combines the advantages of ^{99m}Tc-MIBI and FADS (*19*). When used during early dynamic acquisition, FADS enables detection of abnormal parathyroid gland(s) in the thyroid uptake area and can replace the image subtraction method. Technetium-99m-MIBI is a tracer with excellent physical qualities and, when used alone, avoids the high background and scattering observed with the dual-radioisotope method. With the aim of increasing scintigraphy's sensitivity, SPECT imaging was added to the planar views and FADS with several advantages.

First, SPECT allows better localization of the enlarged glands. The superposition of the two radiomarkers results in more accurate location of the abnormal gland. These more precise scintigraphic results by SPECT have direct surgical consequences because they enable the surgeon to choose the best route of access, particularly in patients with posterior cervico-mediastinal glands. SPECT also obviates the need for surgical exploration in areas where access is difficult, particularly the middle mediastinum. Because of this method, three glands were found in the middle mediastinum in this series of patients, which included a series of 337 patients operated on during the last 2 yr in our hospital, compared to only one gland in a previous series of patients operated on by the same surgical team during the preceding 25 yr (*24*).

Second, SPECT reveals the existence of glands not detected by FADS or planar views. Therefore, the additional use of SPECT increased the sensitivity of FADS and planar views alone from 86% (55/64 glands) to 90.5% (58/64). SPECT appears to be of particular interest in patients undergoing reoperation, in which its sensitivity in the present series increased from 79.5% to 87% (34/39). These results compare favorably with sensitivity values reported by others for patients undergoing reoperation with conventional double-tracer scintigraphy using ^{201}Tl [27% (*25*), 52% (*26*) and 68% (*27*)].

Third, SPECT allows correct interpretation of tracer uptake in the upper mediastinal area, leading to a higher specificity. Because any tomographic image analysis can lead to false-positive results, it is interesting to indicate that no such error was observed in the present series, probably because we had good earlier knowledge of the possible anatomic sites of the ectopic parathyroid glands. Despite the many patients with thyroid nodules and the patient without associated thyroid pathology the number of false-positive FADS results was low. This confirmed that nodule thyroid activity is also decreased as normal thyroid tissue, but sometimes more slowly.

Among the reoperated patients in our series, 66.5% of the abnormal glands found were in an abnormal location, including 25.5% in the mediastinum. This finding agrees with the results from another published series (*3,5–9*). Despite this large proportion of abnormally located glands, particularly in the mediastinum, morbidity was low and the surgical success rate was high, which may be an argument for the use of sophisticated scintigraphic evaluation in difficult surgical decisions.

Analysis of our false-negative results shows that the three abnormal parathyroid glands located outside the thyroid area and not seen on the planar views or tomographic slices were hyperplastic. However, in a previous study (*19*), we showed that

about half of the hyperplastic glands were still visible on the planar view 1 hr after tracer injection compared to more than 80% of adenomas.

CONCLUSION

SPECT increases the sensitivity and specificity of parathyroid scintigraphy. It appears particularly useful for the location of mediastinal glands. Our method, which combines the advantages of ^{99m}Tc-MIBI, FADS and SPECT, allows increased scintigraphic accuracy.

REFERENCES

1. Potts JT, Ackerman IP, Barker CF, et al. Diagnosis and management of asymptomatic primary hyperparathyroidism: consensus development conference statement. *Ann Intern Med* 1991;114:593–597.
2. Norton JA Controversies, advances in primary hyperparathyroidism. *Ann Surg* 1992;215:297–299.
3. Beazley RM, Costa J, Ketcham AS. Reoperative parathyroid surgery. *Am J Surg* 1975;130:427–429.
4. Brennan MF, Marx SJ, Doppman J, et al. Results of reoperation for persistent and recurrent hyperparathyroidism. *Ann Surg* 1981;194:671–676.
5. Granberg P-O, Johansson G, Lindvall N, et al. Reoperation for primary hyperparathyroidism. *Am J Surg* 1982;143:296–300.
6. Wang CA Parathyroid re-exploration. A clinical and pathological study of 112 cases. *Ann Surg* 1977;186,n°2:140–145.
7. Prinz RA, Gamvros OI, Allison DJ, Flechter DR, Lynn AL. Reoperations for hyperparathyroidism. *Surg Gynecol Obstet* 1981;152:760–764.
8. Katz AD, Hopp D Parathyroidectomy. Review of 338 consecutive cases for histology, location and reoperation. *Am J Surg* 1982;144:411–415.
9. Palmer JA, Rosen IB. Reoperative surgery of hyperparathyroidism. *Am J Surg* 1982;144:406–410.
10. Anger HO. Tomography and other depth discrimination techniques. In: Hine GJ, Sorenson JA, eds. *Instrumentation in nuclear medicine*, vol. 2. New York, NY: Academic Press; 1974:61–100.
11. Mathieu L, Budinger TF. Pinhole digital tomography. In: *Proceedings of the First World Congress of Nuclear Medicine*. Tokyo, Japan: 1974:1264–1266.
12. Vogel RA, Kirch D, Lefree M, et al. A new method of multiplanar emission tomography using a seven pinhole collimator and an Anger scintillation camera. *J Nucl Med* 1978;19:648–654.
13. Jarritt PH, Ell PJ, Myers MJ, et al. A new transverse section brain imager for single gamma emitters. *J Nucl Med* 1979;20:319–328.
14. Jarritt PH, Ell PJ. A new emission tomographic body scanner. *Nucl Med Commun* 1980;1:94–101.
15. Budinger TF. Physical attributes of single-photon tomography. *J Nucl Med* 1980;21: 579–592.
16. Cullum ID, Jarritt PH, Ell PH. Performance parameters, minimal detectable lesions and partial volume effects for two emission tomographic body units. *Nucl Med Commun* 1980;1:153.
17. Jaszczak RJ, Chang LT, Murphy PH. SPECT using a multi-slice fan beam collimator. *IEEE Trans Nucl Sci* 1979;26:610–618.
18. Ell PJ, Khan O. Emission computerized tomography: clinical applications. *Semin Nucl Med* 1981;11:50–60.
19. Billotey C, Aurengo A, Najean Y, et al. Identifying abnormal parathyroid glands in the thyroid uptake area using Tc-99m-sestamibi and factor analysis of dynamic structures. *J Nucl Med* 1994;35:1631–1636.
20. Coakley AJ, Kettle AG, Wells CP, et al. Technetium-99m-sestamibi: a new agent for parathyroid imaging. *Nucl Med Commun* 1989;10:791–794.
21. O'Deherty MJ, Kettle AG, Wells CP, et al. Parathyroid imaging with Tc-99m-sestamibi: preoperative localization and tissue uptake studies. *J Nucl Med* 1992;33: 313–318.
22. Geatti O, Shapiro B, Prolo G, et al. Location of parathyroid enlargement by Tc-99m-MIBI and ^{201}Tl scintigraphy, ultrasound and CT [Abstract]. *J Nucl Med* 1992;33:894.
23. Casara D, Rubello G, Saladini G, et al. Preoperative imaging of pathologic parathyroid glands (PG): comparison of Tc-99m-MIBI scintigraphy, Tl-201 scintigraphy, neck echography (NE), computed tomography (CT) and magnetic resonance (MR) [Abstract]. *Eur J Nucl Med* 1992;19:684.
24. Sarfati E, De Ferron P, Gossot D, Assens P, Dubost C. Parathyroid adenoma: atypical sites ectopic or not? *J Chir* 1987;1:24–29.
25. Miller DL, Doppman JL, Shawker, et al. Localization of parathyroid adenomas in patients who have undergone surgery. *Radiology* 1987;162:133–137.
26. Brennan MF, Doppman JL, Kurdy AG, et al. Assessment of techniques for preoperative parathyroid gland localization in patients undergoing reoperation for hyperparathyroidism. *Surgery* 1982;91:6–11.
27. Aufferman W, Gooding GAW, Okerlund MD, et al. Diagnosis of recurent hyperparathyroidism: comparison of MR imaging and other imaging techniques. *Am J Roentgenol* 1988;150:1027–1033.

Bone Scans in Neurofibromatosis: Neurofibroma, Plexiform Neuroma and Neurofibrosarcoma

Richard T. Kloos, Vittoria Rufini, Milton D. Gross and Brahm Shapiro

Division of Nuclear Medicine, Department of Internal Medicine, University of Michigan, and Department of Veterans Affairs Medical Centers, Ann Arbor, Michigan

Neurofibromatosis type 1 or von Recklinghausen's disease is one of the most common autosomal dominant genetic disorders. Between 29% and 77% of patients may suffer from a wide range of skeletal abnormalities and, thus, patients with neurofibromatosis frequently undergo skeletal scintigraphy, at which time the common peripheral nerve soft-tissue tumors that occur in this syndrome (neurofibromas, plexiform neuromas and neurofibrosarcomas) may be demonstrated. **Methods:** Single or multiphase ^{99m}Tc methylenediphosphonate (MDP) bone scans were performed in five patients with neurofibromatosis as part of their clinical evaluation. **Results:** We imaged neurofibrosarcomas in three patients, cutaneous neurofibromas in one patient and a plexiform neuroma in one patient. **Conclusion:** Single- or multiphasic bone scans may localize common soft-tissue tumors in neurofibromatosis.

Received Aug. 21, 1995; revision accepted Dec. 13, 1995.

For correspondence or reprints contact: B. Shapiro, MB, ChB, PhD, University of Michigan Medical Center, Division of Nuclear Medicine, Box 0028, 1500 E. Medical Center Drive, Ann Arbor, MI 48109-0028.

Key Words: bone diseases; neurofibroma; neurofibrosarcoma; peripheral nerve neoplasms

J Nucl Med 1996; 37:1778–1783

Neurofibromatosis type 1 or von Recklinghausen's disease (*1–4*) is one of the most common autosomal dominant disorders with a frequency rate of 1 in 3000 live births, an estimated prevalence of 30 patients per 200,000 population. This disease affects about 100,000 people in the United States with about 50% of cases representing new mutations (*5–8*). The gene responsible for its genesis has recently been mapped and cloned (*9,10*). Affected tissues include those of neuro-ectodermal, mesenchymal and endodermal origins. The phenotypic manifestations are protean and may vary from no more than six café-au-lait spots 15 mm in diameter (5 mm in prepubescent patients) to amongst the most grotesque deforming lesions encountered in clinical medicine (*5–7*). The diagnostic criteria are listed in Table 1. The syndrome of bilateral acoustic